Geophysical Research Letters

RESEARCH LETTER
10.1029/2021GL095697

Special Section:
The Arctic: An AGU Joint Special Collection

North Atlantic Cooling is Slowing Down Mass Loss of Icelandic Glaciers

Brice Noël[1], Guðfinna Aðalgeirsdóttir[2], Finnur Pálsson[2], Bert Wouters[1,3], Stef Lhermitte[3], Jan M. Haacker[3], and Michiel R. van den Broeke[1]

[1]Institute for Marine and Atmospheric Research Utrecht, Utrecht University, Utrecht, The Netherlands, [2]Institute of Earth Sciences, University of Iceland, Reykjavìk, Iceland, [3]Department of Geoscience & Remote Sensing, Delft University of Technology, Delft, The Netherlands

Abstract Icelandic glaciers have been losing mass since the Little Ice Age in the mid-to-late 1800s, with higher mass loss rates in the early 21st century, followed by a slowdown since 2011. As of yet, it remains unclear whether this mass loss slowdown will persist in the future. By reconstructing the contemporary (1958–2019) surface mass balance of Icelandic glaciers, we show that the post-2011 mass loss slowdown coincides with the development of the Blue Blob, an area of regional cooling in the North Atlantic Ocean to the south of Greenland. This regional cooling signal mitigates atmospheric warming in Iceland since 2011, in turn decreasing glacier mass loss through reduced meltwater runoff. In a future high-end warming scenario, North Atlantic cooling is projected to mitigate mass loss of Icelandic glaciers until the mid-2050s. High mass loss rates resume thereafter as the regional cooling signal weakens.

Plain Language Summary Icelandic glaciers are currently losing mass, but with a recent slowdown in the last decade. We show that this slowdown coincides with the development of an area of regional cooling in the North Atlantic Ocean to the south of Greenland, called Blue Blob. Cooling in the Blue Blob has been mitigating atmospheric warming in Iceland since 2011, reducing glacier melt. In a future warmer climate, North Atlantic cooling is projected to persist until the mid-2050s, further slowing down mass loss of Icelandic glaciers. High mass loss resumes thereafter as the regional cooling in the Blue Blob weakens.

Key Points:

- We project daily surface mass balance of Icelandic glaciers at 500 m spatial resolution under a high-end warming scenario until 2100
- We correlate the post-2011 glacier mass loss slowdown with a local cooling in the North Atlantic Ocean
- We predict that local North Atlantic cooling will continue mitigating Icelandic glaciers mass loss until the mid-2050s

Supporting Information:

Supporting Information may be found in the online version of this article.

Correspondence to:

B. Noël,
b.p.y.noel@uu.nl

Citation:

Noël, B., Aðalgeirsdóttir, G., Pálsson, F., Wouters, B., Lhermitte, S., Haacker, J. M., & van den Broeke, M. R. (2022). North Atlantic cooling is slowing down mass loss of Icelandic glaciers. *Geophysical Research Letters*, *49*, e2021GL095697. https://doi.org/10.1029/2021GL095697

Received 18 AUG 2021
Accepted 14 JAN 2022

Author Contributions:

Conceptualization: Brice Noël
Data curation: Brice Noël
Formal analysis: Brice Noël, Michiel R. van den Broeke
Funding acquisition: Brice Noël, Michiel R. van den Broeke
Methodology: Brice Noël, Guðfinna Aðalgeirsdóttir, Finnur Pálsson, Bert Wouters, Stef Lhermitte, Jan M. Haacker, Michiel R. ven den Broeke

1. Introduction

Iceland is located on the Mid-Atlantic Ridge, marking the boundary between the North-American and Eurasian tectonic plates, with numerous active volcanoes and glaciers that cover about 10% of the island surface (Björnsson & Pálsson, 2008). Icelandic glaciers span elevations from sea level up to the highest peaks at ∼2,100 m a.s.l. (above sea level), are 340 m thick on average, and cover an area of roughly 11,000 km^2 (Björnsson & Pálsson, 2008, 2020). Iceland hosts four major ice caps (>500 km^2) including the largest Vatnajökull, seven smaller ice masses (>10 km^2), and about 250 glaciers (Björnsson & Pálsson, 2008). In 2019, their total ice volume was estimated at ∼3,400 km^3, which is sufficient to raise global sea-level by 9 mm if completely melted (Björnsson & Pálsson, 2020; Farinotti et al., 2019). Situated at ∼65°N in the North Atlantic Ocean between the warm Irminger Current to the south, the cold East Greenland and East Icelandic Currents to the northwest and northeast, the island experiences a maritime climate and is home to glaciers among the most sensitive to Arctic warming (Björnsson et al., 2013). Since most Icelandic glaciers terminate on land, mass change is primarily governed by their surface mass balance (SMB), that is, the difference between mass gained from winter snowfall and mass lost from meltwater runoff in summer (Figure 1b). Additional processes including basal melting from volcanic eruptions, geothermal heat and mass lost from glacier calving in pro-glacial lakes also contribute to the mass balance (Jóhannesson et al., 2020), but these are assumed to be small compared to the SMB contribution (Björnsson et al., 2013). As contemporary precipitation has remained mostly unchanged in Iceland, changes in glacier SMB are primarily driven by trends in atmospheric temperature, resulting in fluctuations of meltwater runoff (Björnsson et al., 2013). Superimposed on this, major volcanic eruptions cause high incidental SMB variability as a result of large-scale deposition of dark tephra (ashes) on the brighter snow and ice that amplifies surface melt through a strong albedo effect (Björnsson et al., 2013; Box et al., 2012; Gascoin et al., 2017; Gunnarsson et al., 2021; Schmidt et al., 2017). Icelandic glaciers have been losing mass since their peak extent at the end of the Little Ice Age in the mid-to-late 1800s (Aðalgeirsdóttir et al., 2020), with accelerated mass loss following the recent rapid Arctic warming (Meredith et al., 2019). Peak mass loss occurred in 2010 concurrent with the massive

Project Administration: Brice Noël, Michiel R. van den Broeke
Writing – original draft: Brice Noël
Writing – review & editing: Brice Noël, Guðfinna Aðalgeirsdóttir, Finnur Pálsson, Bert Wouters, Stef Lhermitte, Jan M. Haacker, Michiel R. van den Broeke

eruption of Eyjafjallajökull that covered surrounding ice caps with dark volcanic tephra, reducing surface albedo (Gudmundsson et al., 2012; Möller et al., 2019). In sharp contrast, mass loss has slowed down since 2011 (Aðalgeirsdóttir et al., 2020; Ciraci et al., 2020; Hock et al., 2019; Wouters et al., 2019), but as of yet little is known about whether this slowdown is temporary, if it will persist or further strengthen in the future.

To address this, we use the Regional Atmospheric Climate Model RACMO2.3 (see Section 2.1). For the recent past (1958–2019), the model is forced by climate reanalyses including the latest product of the European Centre for Medium-Range Weather Forecasts (ECMWF) ERA5 (Hersbach et al., 2020; RACMO2.3-ERA henceforth; Noël et al., 2015). For projections throughout the 21st century (1958–2099), RACMO2.3 is forced by the output of the Community Earth System Model CESM2 (see Section 2.2) under a high-end Shared Socioeconomic Pathway SSP5-8.5 emission scenario (RACMO2.3-CESM2 henceforth; Noël et al., 2021). Using a high-end emission scenario enables us to explore the response of Icelandic glaciers to unmitigated atmospheric warming until the end of the century. Daily SMB and its components, including snowfall and rainfall, surface melt, refreezing, retention and runoff, are further statistically downscaled from the output of RACMO2.3 at 11 km to a gridded glacier mask (RGI Consortium, 2017) and digital elevation model (Porter et al., 2018) re-sampled to 500 m horizontal resolution (Figure S1a in Supporting Information S1). Statistical downscaling (Noël et al., 2016) corrects daily melt and runoff for elevation differences on the relatively coarse 11 km grid using modelled elevation gradients, and for underestimated bare ice and volcanic tephra albedo using remotely sensed measurements from the Moderate Resolution Imaging Spectroradiometer (MODIS; Figure S1b in Supporting Information S1; see Section 2.3). We use this new, daily data set, thoroughly evaluated using a combination of in situ (see Section 2.4) and remote sensing measurements (see Section 2.5), that reconstructs the recent (1958–2019) and projects the future (1958–2099) SMB of Icelandic glaciers at 500 m spatial resolution to explore whether the post-2011 mass loss slowdown will further persist under extreme warming in the course of the 21st century.

2. Materials and Methods

2.1. Regional Atmospheric Climate Model

We use output of the Regional Atmospheric Climate Model (RACMO2.3) over a domain including Greenland, the Canadian Arctic, Svalbard and Iceland at 11 km spatial resolution for the period 1958–2019 (Noël et al., 2015). The model incorporates the dynamical core of the High Resolution Limited Area Model (HIRLAM; Undèn et al., 2002) and the physics package cycle CY33r1 of the European Centre for Medium-Range Weather Forecasts-Integrated Forecast System (ECMWF-IFS, 2008). The model is specifically adapted to represent surface processes in glaciated regions, and includes a 40-layer snow module simulating melt, percolation, retention and refreezing into snow layers, and subsequent surface runoff (Ettema et al., 2010). RACMO2.3 represents dry-snow densification (Ligtenberg et al., 2011), drifting snow erosion (Lenaerts et al., 2012), and snow albedo based on grain size, cloud optical thickness, solar zenith angle, and impurity content (soot; Van Angelen et al., 2012). Here we estimate the SMB of Icelandic glaciers as the local (kg m^{-2}) and the spatially integrated (Gt yr^{-1}) sum of,

$$SMB = PR - RU - SU - ER \quad (1)$$

where PR is total precipitation, that is, the sum of snowfall (SF) and rainfall (RA) precipitation, RU is the surface runoff, SU and ER are the total sublimation and the erosion of drifting snow, which are small and do not significantly contribute to SMB. Surface runoff is estimated as the fraction of rain and melt (ME) that is not retained or refrozen (RF) in firn as,

$$RU = ME + RA - RF \quad (2)$$

The above definition of SMB including 'internal accumulation' from refreezing and retention (RF), is referred to as 'climatic mass balance' in (Cogley et al., 2011).

For the contemporary climate, RACMO2.3 is forced by ERA-40 (1958–1978; Uppala et al., 2005), ERA-Interim (1979–2018; Dee et al., 2011) and ERA5 (2019; Hersbach et al., 2020) reanalyses within a 24-grid-cell-wide relaxation zone at the model lateral boundaries. Forcing consists of temperature, pressure, specific humidity, wind speed and direction being prescribed at the 40 model atmospheric levels every 6 hr. Upper atmospheric relaxation is active (Van de Berg & Medley, 2016). Sea ice extent and sea surface temperature are also prescribed from the reanalyses on a 6-hourly basis. The snowpack is initialised in September 1957 using snow temperature

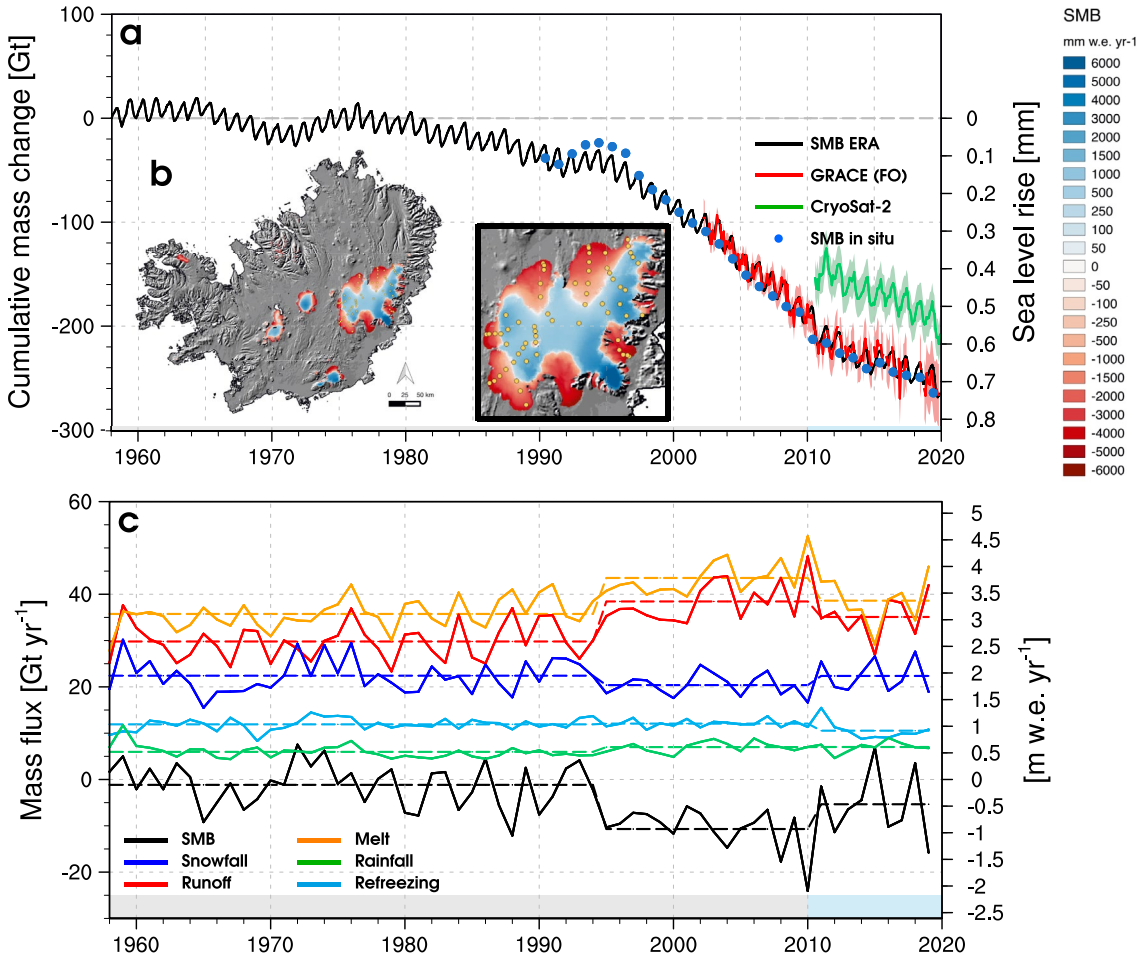

Figure 1. (a) Time series of monthly cumulative SMB integrated over all Icelandic glaciers and ice caps (black) from RACMO2.3-ERA at 500 m resolution (1958–2019). Observed mass change integrated over the three largest Icelandic ice caps using annual in situ SMB measurements (blue) (Aðalgeirsdóttir et al., 2020), and monthly GRACE(-FO) (red) and CryoSat-2 (green) are shown for comparison. CryoSat-2 mass change is offset by 50 Gt for clarity. Uncertainties in the GRACE and CryoSat-2 products are shown as coloured bands (see Section 2.5). Mass loss is converted into mm sea level rise equivalent (right axis). (b) SMB of Icelandic glaciers at 500 m spatial resolution, averaged for the period 1958–2019. The inset map locates 64 mass balance measurement sites on the main Vatnajökull ice cap (yellow dots) (see Section 2.4). (c) Time series of glacier-integrated SMB components from RACMO2.3-ERA at 500 m resolution for the period 1958–2019. Dashed coloured lines represent SMB components averaged for the key periods 1958–1994, 1995–2010 and 2011–2019. Note that modelled cumulative mass change in (b) does not consider non-surface mass balance processes such as basal melt and calving (Jóhannesson et al., 2020).

and density profiles from the offline Firn Densification Model (FDM; Ligtenberg et al., 2018). Ice albedo is prescribed from the 500 m Moderate-resolution Imaging Spectroradiometer (MODIS) 16-day surface albedo product (MCD43A3) as the lowest 5% annual values averaged for the period 2000–2015, and clipped between 0.30 for dark bare ice and 0.55 for clean bright ice under perennial snow. For future climate, RACMO2.3 is forced by CESM2.

2.2. Community Earth System Model

We use the Coupled Model Intercomparison Project Phase 6 (CMIP6) Community Earth System Model (CESM2) to project the Earth's climate on the global scale throughout the 21st century. The model includes the Community Atmosphere Model version 6 (CAM6; Gettelman et al., 2019), the Parallel Ocean Program model version 2.1 (POP2.1; Smith et al., 2010), the Los Alamos National Laboratory Sea Ice Model version 5.1 (CICE5.1; Bailey et al., 2018), the Community Land Model version 5 (CLM5; Lawrence et al., 2019), and the Community Ice Sheet Model version 2.1 (CISM2.1; Lipscomb et al., 2019) to simulate interactions between atmosphere-ocean-land with sea ice dynamics and snow/ice surface processes in a fully-coupled fashion. Here all modules are active

except for ice dynamics, that is, excluding calving processes and subsequent glacier thinning and retreat. The model runs at a spatial resolution of 0.9 × 1.25° (∼111 km) and exclusively prescribes land use changes, atmospheric greenhouse gas and aerosol emissions (Eyring et al., 2016). A climate projection from CESM2 under a high-end emission scenario (SSP5-8.5) is used to force RACMO2.3 at 11 km every 6 hr throughout the 21st century (1958–2099). Sea ice extent and sea surface temperature are also prescribed from CESM2 on a 6-hourly basis. The product is further statistically downscaled to 500 m spatial resolution.

2.3. Statistical Downscaling

To accurately resolve SMB patterns over the relatively small glaciers of Iceland, the daily output of RACMO2.3 forced by ERA reanalyses (1958–2019) and CESM2 (1958–2099) are statistically downscaled to a 500 m ice mask derived from the Randolph Glacier Inventory (RGI Consortium, 2017) version 6 and the 100 m spatial resolution ArcticDEM (Porter et al., 2018), re-sampled onto a 500 m grid (Figure S1a in Supporting Information S1). The downscaling procedure corrects individual SMB components (except for total precipitation), that is, primarily surface melt and runoff, for elevation and albedo differences on the relatively coarse model grid at 11 km resolution. These corrections reconstruct individual SMB components on the 500 m topography using daily-specific elevational gradients estimated at 11 km. Runoff is further adjusted using a re-sampled 500 m MODIS 16-day product providing albedo records on annual basis for the period 2000–2019. Interannual fluctuations in the MODIS albedo product are essential to capture the high SMB variability resulting from large-scale deposition of dark tephra on snow and ice following major volcanic eruptions in the period 2000–2019 (Schmidt et al., 2017), for example, Eyjafjallajökull in 2010 (Figure 1c). For the pre-2000 and post-2019 periods, we use the MODIS albedo product averaged for 2000–2019, excluding the outlier eruption year 2010 (Figure S1b in Supporting Information S1). In line with Gascoin et al. (2017) and Gunnarsson et al. (2021), the minimum albedo in MODIS imageries for tephra-covered snow in the accumulation zone is set to 0.30, while for tephra-covered bare ice in the ablation zone, the minimum is set to 0.15. Total precipitation is bilinearly interpolated from the 11 km onto the 500 m grid without additional corrections. The statistical downscaling technique is further described in (Noël et al., 2016).

2.4. In Situ Records

We use 1196 in situ surface mass balance measurements covering the period 1991–2019 and collected at ∼65 sites (Figure 1c) across the main Vatnajökull ice cap (Pálsson et al., 2020). Annual mass balance is estimated from surface height change between consecutive stake measurements in September, while summer and winter balances are estimated from surface height change between consecutive stake measurements in May-September and September-May, respectively, considering the density of the ice/snow that was lost/gained. For a meaningful comparison, modelled SMB is summed over the exact overlapping period in days. Since 'internal accumulation' is not measured by stakes, while it is included in our model SMB definition (Equation 2), we subtract modelled refreezing and retention from the downscaled SMB in the accumulation zone, that is, where SMB > 0 on average for 1958–2019. For local comparison with stake measurements, we selected the downscaled grid cell with the smallest elevation difference among the closest pixel and its eight adjacent neighbours. We rejected one site (HOSP) situated outside the Randolph Glacier Inventory ice mask, and three other sites (BR0-BR1-BR2, see inset map in Figure S2c in Supporting Information S1) situated outside the RACMO2.3 ice mask at 11 km in a sector of Vatnajökull that experiences the highest mass loss rates (Pálsson et al., 2020). The latter three sites are shown for illustration but were not considered in the regression statistics (red dots in Figures S2a, S2b and S2d in Supporting Information S1).

For comparison of spatially integrated SMB, we also use time series of annual mass change (blue dots in Figure 1a) integrated over the three largest Icelandic ice caps, that is, namely Vatnajökull (glaciological years 1991/1992–2018/2019), Hofsjökull (1988/1989–2018/2019) and Langjökull (1995/1996–2018/2019). This time series is further described in Aðalgeirsdóttir et al. (2020).

To evaluate modelled 2 m air temperature (T2m) in RACMO2.3-ERA, we use 51,833 daily in situ measurements from 27 automatic weather stations (AWS) installed on the four main Icelandic ice caps (Figure S2e in Supporting Information S1). Measurements cover the period 1994–2019 and span the summer season, but sometimes further extend from mid-April to end of December. We find good agreement between modelled and measured

2 m air temperature ($R^2 = 0.84$) with a relatively small cold bias (−0.48°C, i.e., mean difference between model and observations) and small RMSE (2.15°C), highlighting the ability of RACMO2.3 to represent the near-surface temperature above Icelandic glaciers (Figure S2f in Supporting Information S1).

2.5. Remote Sensing Records

We use both GRACE(-FO) mass change time series for the period 2002–2019 (Wouters et al., 2019) and elevation changes derived from CryoSat-2 (2011–2019). A swath retrieval algorithm similar to Garcia-Mondéjar et al. (2019) is used to estimate surface elevation from CryoSat-2 SARIn data (Baseline D). Local surface topography from the ArcticDEM mosaic at 100 m resolution (Porter et al., 2018) is then subtracted from our CryoSat-2 estimate. After outliers have been excluded recursively, we derive an average elevation difference between the two products in 50 m elevation bands within individual glacier drainage basins of the Randolph Glacier Inventory version 6 (RGI Consortium, 2017). Small basins were grouped to ensure sufficient data coverage. Monthly volume anomalies (with respect to an arbitrary mean) are obtained by multiplying the elevation difference by the basin hypsometric area. When insufficient observations are available within a basin for a given month, data gaps are filled by linear temporal interpolation of up to 2 months. Where this is not possible, the elevation change rates are interpolated between elevation bands using a fitted polynomial. Remaining data gaps are filled by assuming an average trend from neighouring basins in a same elevation band. Mass change is calculated from the volume anomalies assuming constant density profiles. Volumes above 1,200 m a.s.l. are multiplied by a firn density of 650 kg m^{-3} and volumes below this elevation by the ice density of 900 kg m^{-3}. Uncertainties in the GRACE and CryoSat-2 products are estimated from Wouters et al. (2019) as being one standard deviation (17.9 Gt per month) of the 2011–2019 mass change (Figure 1a and Figure S2b in Supporting Information S1), respectively.

2.6. Model Uncertainty

The model annual SMB uncertainty (σ) is estimated at 2.5 Gt yr^{-1} on average for the period 1958–2019. Following Noël et al. (2019), the uncertainty is obtained by integrating the conservative 10% (136 mm w.e.) and 20% (401 mm w.e.) SMB uncertainty in RACMO2.3 over the long-term accumulation ($A_{\text{accum.}} = 5{,}900$ km^2) and ablation zones ($A_{\text{abla.}} = 5{,}600$ km^2) of Icelandic glaciers.

$$\sigma = \sqrt{\left(\frac{136 \times A_{\text{accum.}}}{1e^6}\right)^2 + \left(\frac{401 \times A_{\text{abla.}}}{1e^6}\right)^2} \tag{3}$$

A similar uncertainty is derived from model comparison with seasonal in situ measurements (see Figures S2c and S2d in Supporting Information S1). Compared to stake measurements, the SMB product shows a mean bias of 310 mm w.e. in winter (210 mm w.e. in summer), that is, representative of snowfall accumulation (runoff ablation). Integrated over the long-term accumulation (ablation) area of Icelandic glaciers, this results in an annual SMB uncertainty of 2.2 Gt yr^{-1} (Figures S2c and S2d in Supporting Information S1). Compared to remotely sensed estimates from GRACE ($R^2 = 0.98$) and CryoSat-2 ($R^2 = 0.93$), we find a mean modelled SMB bias of 0.61 and 0.06 Gt per month (Figure S2b in Supporting Information S1).

3. Results

The present-day SMB product has been thoroughly evaluated using a combination of in situ and remote sensing measurements, showing excellent agreement ($0.81 < R^2 < 0.98$; Figures S2a and S2b in Supporting Information S1). In situ measurements consist of 1,196 records of annual, winter and summer balance from ~65 sites located on the main Vatnajökull ice cap (1991–2019; Figure 1b and Figures S2a, S2c and S2d in Supporting Information S1; Aðalgeirsdóttir et al., 2020; Pálsson et al., 2020). The evaluation of summer and winter balances suggest a small underestimation of winter accumulation (310 mm w.e. yr^{-1} on average, shown in Figure S2c in Supporting Information S1), that is partly compensated by an underestimation of summer ablation (210 mm w.e. yr^{-1}, shown in Figure S2d in Supporting Information S1). The ablation underestimation can be partly ascribed to the fact that RACMO2.3 at 11 km resolution does not well capture high melt rates of small, low-lying outlet glaciers, especially in the southeast of Vatnajökull where they almost reach sea level. In addition, the SMB product does not account for non-surface mass balance processes (e.g., basal melt, calving) that are currently estimated

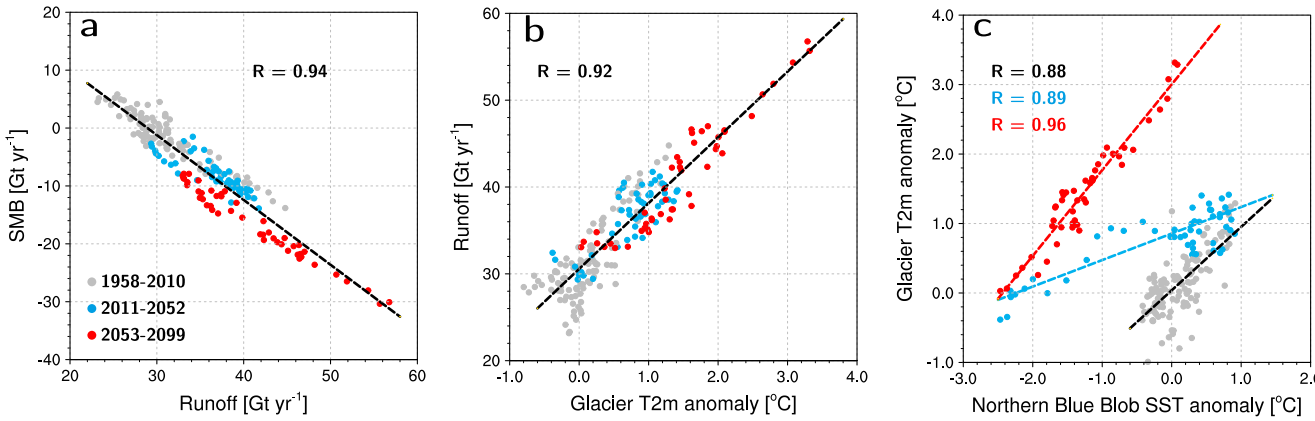

Figure 2. (a) Correlation between glacier-integrated runoff and SMB. (b) Correlation between anomalies in 2 m air temperature (T2m) averaged over the glacier area of Iceland and runoff. (c) Correlation between anomalies in sea surface temperature (SST) of the Northern Blue Blob (NBB, blue contour in Figure 3) and in glacier T2m. Anomalies are calculated relative to the period 1958–1994. Coloured dots represent three key stages: 1958–2010 (grey), 2011–2052 (cyan) and 2053–2099 (red). Coloured dashed lines show linear regressions for the different stages; the corresponding correlation coefficients (R) are listed. A 5-yr running mean is applied in (a)–(c).

to contribute ~2 Gt yr^{-1} (Jóhannesson et al., 2020). To further evaluate glacier-integrated SMB, the downscaled product is also compared to remotely sensed mass change estimates from the Gravity Recovery and Climate Experiment (GRACE) satellite, its Follow On mission (GRACE-FO), as well as CryoSat-2 since 2002 (Figure 1a and Figure S2b in Supporting Information S1). There is a good agreement between the downscaled SMB product and both satellite estimates, and the resulting total bias is of similar order as the non-surface mass balance contribution (Jóhannesson et al., 2020). In spite of the good agreement with in situ and satellite gravimetry and altimetry products, it is important to note that (large) local uncertainties in individual SMB components in space and time remain. These uncertainties must be addressed by enhancing the amount of available measurements through continued survey of Icelandic glaciers. Nonetheless, our new present-day SMB product accurately captures both the long-term mass loss trend and the seasonal cycle of winter mass gains and summer mass losses (Figure 1a).

Historical records revealed that Icelandic glaciers have been losing mass since the Little Ice Age in the mid-to-late 1800s and throughout the 20th century (Aðalgeirsdóttir et al., 2020; Björnsson et al., 2013). For the contemporary climate, our results show that Icelandic glaciers reached an approximate mass balance between the late 1950s and the mid-1990s (Figure 1a), in line with the above previous studies (Aðalgeirsdóttir et al., 2020; Björnsson et al., 2013). A shift to negative mass balance arises after 1995, in close agreement with independent in situ measurements (Aðalgeirsdóttir et al., 2020). Satellite gravimetry and altimetry confirm this negative trend from the early 2000s until 2010 (Box et al., 2018; Ciraci et al., 2020; Gardner et al., 2013; Jacob et al., 2012; Nilsson et al., 2015; Schrama et al., 2014; Siemes et al., 2013; Sørensen et al., 2017; Von Hippel & Harig, 2019; Wouters et al., 2008, 2019; Zemp et al., 2019; Table S1 in Supporting Information S1). In contrast, the year 2011 marks the onset of a mass loss slowdown (Figure 1a) (Aðalgeirsdóttir et al., 2020; Foresta et al., 2016; Wouters et al., 2019). Drivers of these mass change variations can be identified using our high-resolution SMB product (Figure 1c). In the period 1958–1994, total precipitation (28.4 Gt yr^{-1} on average), that is, the sum of snowfall and rainfall, compensated for the mass lost from surface runoff (29.8 Gt yr^{-1}), resulting in a SMB close to zero (-1.2 ± 2.5 Gt yr^{-1}; Table S2 in Supporting Information S1). Following a 0.6°C atmospheric warming in 1995–2010 (orange line in Figure 4b), runoff increased by ~30% (+8.6 Gt yr^{-1}; 1995–2010 minus 1958–1994) due to enhanced melt (+7.4 Gt yr^{-1}) and rainfall (+1.0 Gt yr^{-1}), initiating significant mass loss in the mid-1990s (-10.7 ± 2.5 Gt yr^{-1} for 1995–2010; Table S2 in Supporting Information S1). From 2011 onward, runoff decreased by 3.3 Gt yr^{-1} (-12%) compared to the period 1995–2010, resulting in the post-2011 slowdown that essentially halved the mass loss relative to 1995–2010 (-5.3 ± 2.5 Gt yr^{-1} for 2011–2019; Table S2 in Supporting Information S1).

Linear regression shows that variations in the SMB of Icelandic glaciers are mainly driven by fluctuations in meltwater runoff ($R = 0.94$ in Figure 2a). In turn, runoff varies linearly as a function of spatially averaged glacier 2 m air temperature (T2m; $R = 0.92$ in Figure 2b). As shown for the Greenland ice sheet (Fausto et al., 2016), the latter relationship reflects that although absorbed shortwave radiation is the main energy source for melt in Iceland, fluctuations in downward longwave radiation and sensible heat flux following the advection of cold/warm

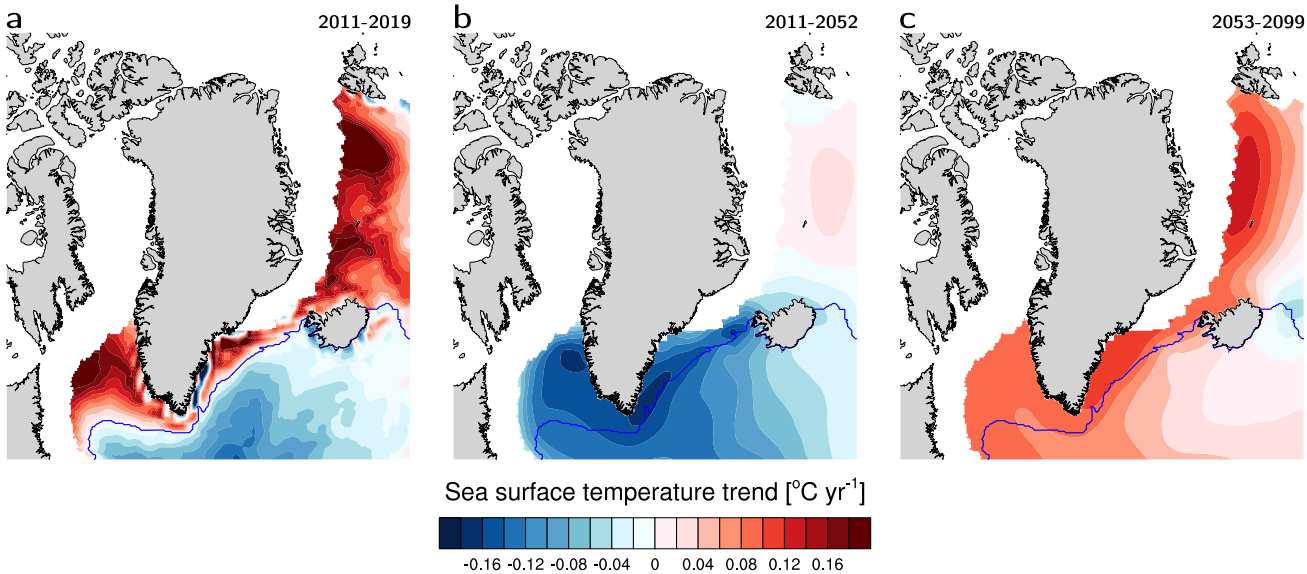

Figure 3. Sea surface temperature trend (a) observed in ERA reanalyses over 2011–2019; predicted by CESM2 in (b) 2011–2052 and (c) 2053–2099. The blue contour outlines the area as assumed to represent the Northern Blue Blob (NBB) in the North Atlantic Ocean, that is, negative SST trend in the ERA reanalyses (2011–2019). The southern and eastern boundaries of the NBB match the figure borders. Only sea-ice free pixels were considered.

air masses explain most of the interannual variability in 2 m air temperature above glaciers, and thus mass change. As a third connection, we find that modelled Icelandic glacier 2 m air temperature strongly correlates with sea surface temperature (SST) measured by ERA reanalyses in the North Atlantic Ocean ($R = 0.88$ for the period 1958–2010 in Figure 2c), notably in a region south of Greenland called the Blue Blob (Josey et al., 2017). Here, we focus on the northern part of this cooling area, referred to as Northern Blue Blob (NBB), fringing the southern tip of Greenland and Iceland (blue contour in Figure 3a). As a result, SMB and runoff from Icelandic glaciers also strongly correlate with measured sea surface temperature in the NBB area (Figure S4a in Supporting Information S1). Surface temperature in the NBB remained almost unchanged until the mid-1990s (grey line in Figure 4b) and thereafter started to increase simultaneously and at the same rate as Iceland glacier 2 m air temperature (+0.07°C yr^{-1}; orange line in Figure 4b). After 2011, cooling in the NBB (locally −0.15°C yr^{-1} in Figure 3a) strongly reduced atmospheric warming above Icelandic glaciers (Figure 4b), hence decreasing meltwater runoff (Figure 1c). We conclude that the post-2011 development of the Blue Blob resulted in the slowdown of glacier mass loss in Iceland (Figure 1a).

To predict the influence of the North Atlantic Ocean temperature evolution on the glacier mass balance throughout the 21st century, we use downscaled output of RACMO2.3-CESM2 under a high-end warming scenario (Figure 4a). Using such a scenario enables us to explore the glacial response to the most extreme future atmospheric and oceanic temperature forcing. First we ascertained that RACMO2.3-CESM2 reproduces (1) Icelandic glaciers to be in approximate mass balance before 1995, (2) the onset of mass loss in the period 1995–2010, and (3) the post-2011 slowdown (Figure 4a). In addition, we confirmed that RACMO2.3-CESM2 realistically captures the spatial correlations between sea surface temperature in the NBB and Iceland glacier 2 m air temperature (Figures S3a and S3b in Supporting Information S1). It is important to note that CESM2 does not assimilate observations, as opposed to ERA reanalyses, and interannual variability will consequently differ between the two forcings. Therefore, it is to be expected that both spatial correlations (Figures S3a, S3b and S4a, S4b in Supporting Information S1) and modelled SMB from RACMO2.3-CESM2 and RACMO2.3-ERA are slightly different (~4 Gt on average for 1958–2019; Figure 4a). Nevertheless, both products show similar correlation patterns, SMB variability and trend (−0.2 Gt yr^{-2} for 1958–2019). Under the SSP5-8.5 scenario, RACMO2.3-CESM2 projects sustained cooling in the NBB area from 2011 to 2052 (Figure 3b). By the mid-2050s, the NBB area is predicted to cool by ~3°C compared to 1958–2010 (cyan dots in Figure 2c and black line in Figure 4b), resulting in a ~2°C decrease in glacier 2 m air temperature ($R = 0.89$; cyan dots in Figure 2c and red line in Figure 4b).

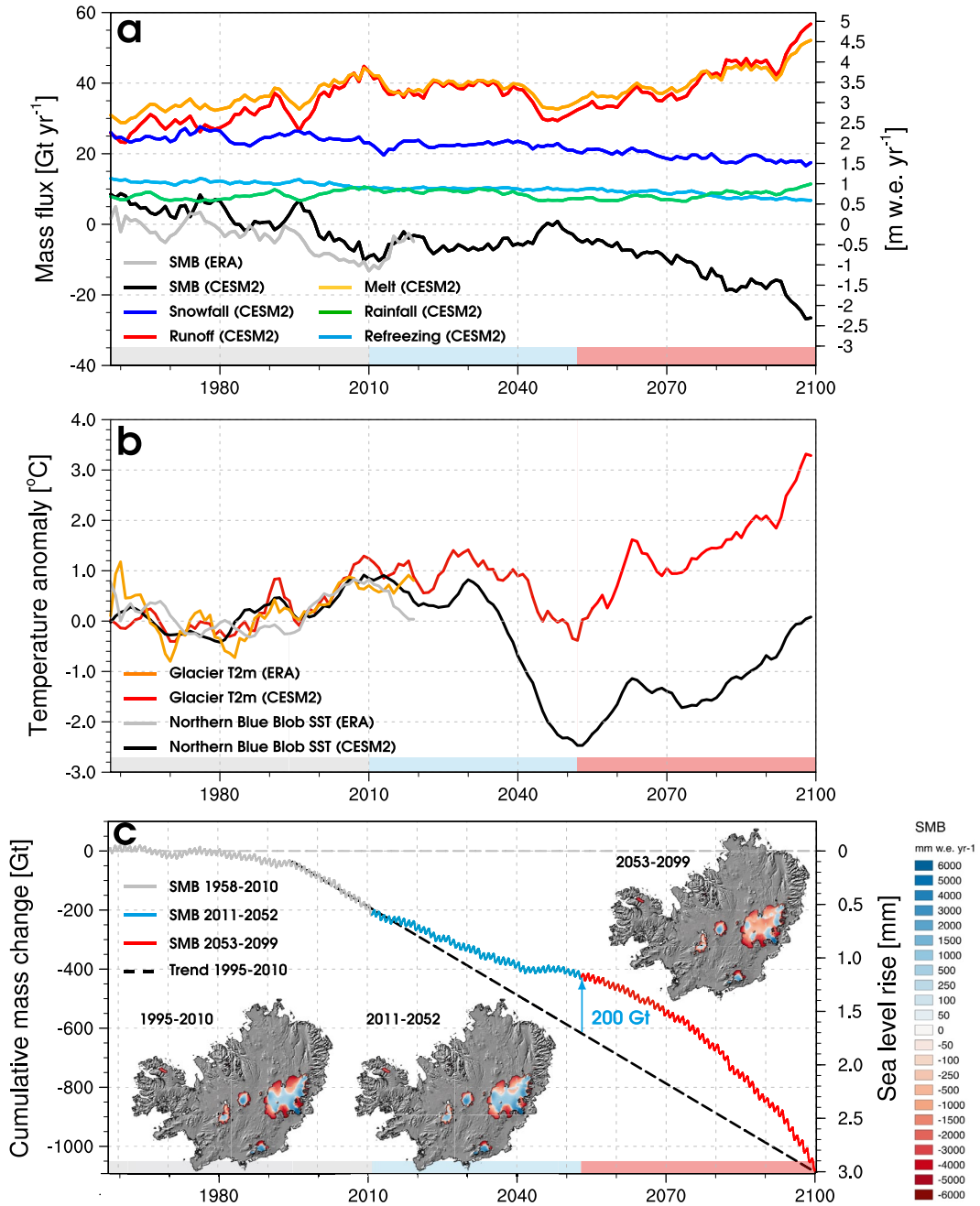

Figure 4. (a) Time series of glacier-integrated SMB components from RACMO2.3-CESM2 at 500 m resolution under a high-end warming scenario (1958–2099). Glacier-integrated SMB from RACMO2.3-ERA is shown in grey for comparison (1958–2019). (b) Anomalies in glacier T2m and in Northern Blue Blob (NBB, blue contour in Figure 3) SST from RACMO2.3-ERA (orange and grey) and CESM2 (red and black) relative to the period 1958–1994. (c) Time series of monthly cumulative glacier-integrated mass change from 1958 to 2099 under a high-end warming scenario. Three mass balance stages are distinguished: 1958–2010 (grey), 2011–2052 (cyan) and 2053–2099 (red). Coloured bands highlight the three stages. The dashed black line extrapolates the 1995–2010 mass loss trend until 2099. Mass loss is converted into mm sea level rise equivalent (right axis). Inset maps represent SMB of Icelandic glaciers averaged for 1995–2010, 2011–2052 and 2053–2099. A 5-yr running mean is applied in (a) and (b).

4. Discussion and Conclusions

We interpret the asymmetric cooling between ocean and atmospheric temperature as the superposition of a background warming trend with a superimposed regional perturbation (Figure 2c). This mechanism is illustrated by

idealised linear temperature regressions in Figure S5 in Supporting Information S1. Since the mid-1990s, Icelandic glaciers and the North Atlantic Ocean have experienced a similar background warming (red line in Figure S5a in Supporting Information S1). Superimposed on this, the North Atlantic is currently undergoing and will undergo a pronounced regional cooling in the Blue Blob area from 2011 until the mid-2050s (blue line in Figure S5a in Supporting Information S1). As the regional temperature decline exceeds the background warming, this results in a net surface cooling in the NBB area (black line in Figure S5a in Supporting Information S1). This local oceanic cooling is currently observed in the North Atlantic (Figure 3a), and has been linked to the development of the Warming Hole, that is, a long-term (multi-decadal) cooling of the North Atlantic Ocean that has been ascribed to a potential weakening of the Atlantic Meridional Overturning Circulation (AMOC) (Caesar et al., 2018; Keil et al., 2020; Rahmstorf et al., 2015; Zhu & Liu, 2020). While the significance of the long-term Warming Hole cooling and the role played by the AMOC remain uncertain (Fox-Kemper et al., 2021), the strong cooling recently observed in the Blue Blob is strengthened by regional atmospheric cooling resulting from interannual variability of the North Atlantic Oscillation (Josey et al., 2017). Applying a linear fit to the data suggests that Icelandic glaciers experience only 60% of the NBB cooling signal. We interpret this as atmospheric cold content being partly dissipated by the advection of air masses between the NBB and Iceland (orange line in Figure S5a in Supporting Information S1). Consequently, the decline in glacier 2 m air temperature is approximately half that of sea surface temperature in the NBB (Figure 4b), explaining the asymmetrical (z-shaped) correlation (cyan dots in Figure 2c and Figure S5b in Supporting Information S1). After the mid-2050s, North Atlantic cooling is projected to halt in CESM2, so that the background warming signal prevails again in the NBB (Figure 3c). This results in a parallel increase of sea surface and Iceland glacier 2 m air temperature by ∼3.5°C until 2100 ($R = 0.96$; red dots in Figures 2c and 4b). In line with our results, Gervais et al. (2018) projected a persistent cooling in the NBB until the 2050s, followed by a temperature increase under a high-end warming scenario (see their Figure 4a). However, they do not identify the driving processes of the latter warming. We hypothesise that potential mechanisms include reduced cold water and sea ice transport from the Labrador Sea and Fram Strait into the NBB area following atmospheric warming in the second half of the century.

Based on past and projected sea surface temperature fluctuations in the NBB (black line in Figure 4b), we identify three different stages for the mass balance of Icelandic glaciers under a high-end emission scenario. In 1958–2010 (grey shade in Figure 4), the 2 m air temperature over Icelandic glaciers increases according to the background warming (Figure 3b), enhancing runoff (Figure 4a) and bringing Icelandic glaciers from approximate mass balance (1958–1994) to mass loss (1995–2010; grey line in Figure 4c). In 2011–2052 (cyan shade in Figure 4), Icelandic glacier mass loss slows down, the result of pronounced cooling in the NBB that reduces runoff and even returns glaciers to a state of approximate mass balance in the late 2040s (cyan line in Figure 4c). From the mid-2050s onward, warming is projected to prevail again in the NBB, enhancing runoff and resuming mass loss (red line in Figure 4c). As a result, Icelandic glaciers could lose about 30% of their total volume by 2100 (Figure 4c). If, as we project, the slowdown of mass loss persists until the 2050s, Icelandic glaciers could preserve ∼200 Gt of ice (or 5% of the total volume) by the mid-2050s relative to a trajectory of sustained mass loss at the 1995–2010 rate (dashed line in Figure 4c). Under a high-end warming scenario, mass loss accelerates again in the mid-2050s (-14.0 ± 2.5 Gt yr^{-1} for 2053–2099). At the latter mass loss rate, and without additional feedbacks, Icelandic glaciers could completely vanish by the end of the 23rd century.

Conflict of Interest

The authors declare no conflicts of interest relevant to this study.

Data Availability Statement

Data required to reproduce the figures and tables presented in the study are available on Zenodo (https://doi.org/10.5281/zenodo.5836476). Data include (1) time series of reconstructed (RACMO2.3-ERA, 1958–2019) and projected (RACMO2.3-CESM2, 1958–2099) annual SMB components spatially-integrated over Icelandic glaciers: SMB, snowfall, rainfall, runoff, total melt and refreezing expressed in Gt per year; (2) time series of monthly SMB in Gt per month (January 1958–December 2099); (3) annual SMB maps from RACMO2.3-ERA (1958–2019) and RACMO2.3-CESM2 (1958–2099) in mm w.e. per year; and (4) time series of annual mean 2 m air temperature (T2m) above Icelandic glaciers and sea surface temperature (SST) in the Northern Blue Blob

(NBB) in K from RACMO2.3-ERA (1958–2019) and RACMO2.3-CESM2 (1958–2099). ERA reanalyses are available from the European Centre for Medium-Range Weather Forecasts (ECMWF; https://www.ecmwf.int/en/forecasts/datasets/browse-reanalysis-datasets). These reanalyses are discussed in Uppala et al. (2005) (ERA-40), Dee et al. (2011) (ERA-Interim) and Hersbach et al. (2020) (ERA5).

Acknowledgments
B. Noël was funded by the NWO VENI grant VI.Veni.192.019. B. Wouters and J. M. Haacker were funded by NWO VIDI Grant 016.Vidi.171.063. This publication was also supported by the Netherlands Earth System Science Centre (NESSC) and PROTECT. This project has received funding from the European Union's Horizon 2020 research and innovation programme under grant agreement No 869 304, PROTECT contribution number 28.

References

Aðalgeirsdóttir, G., Pálsson, F., Thorsteinsson, T., Magnússon, E., Belart, J. M. C., Jóhannesson, T., et al. (2020). Glacier changes in Iceland from 1890 to 2019. *Frontiers in Earth Science*, *8*(523646), 1–15. https://doi.org/10.3389/feart.2020.523646

Bailey, D., Hunke, E., DuVivier, A., Lipscomb, B., Bitz, C., Holland, M., et al. (2018). CESM CICE5 Users Guide, Release CESM CICE5. *Documentation and Software User's Manual from Los Alamos National Laboratory* (pp. 1–41). Retrieved from http://www.cesm.ucar.edu/models/cesm2/sea-ice/

Björnsson, H., & Pálsson, F. (2008). Icelandic glaciers. *Jokull*, *58*, 365–386.

Björnsson, H., & Pálsson, F. (2020). Radio-echo soundings on Icelandic temperate glaciers: History of techniques and findings. *Annals of Glaciology*, *61*(81), 25–34. https://doi.org/10.1017/aog.2020.10

Björnsson, H., Pálsson, F., Gudmundsson, S., Magnússon, E., Aðalgeirsdóttir, G., Jóhannesson, T., et al. (2013). Contribution of Icelandic ice caps to sea level rise: Trends and variability since the Little Ice Age. *Geophysical Research Letters*, *40*(8), 1546–1550. https://doi.org/10.1002/grl.50278

Box, J. E., Colgan, W. T., Wouters, B., Burgess, D. O., O'Neel, S., Thomson, L. I., & Mernild, S. H. (2018). Global sea-level contribution from Arctic land ice: 1971–2017. *Environmental Research Letters*, *13*(12). 125012. https://doi.org/10.1088/1748-9326/aaf2ed

Box, J. E., Fettweis, X., Stroeve, J. C., Tedesco, M., Hall, D. K., & Steffen, K. (2012). Greenland ice sheet albedo feedback: Thermodynamics and atmospheric drivers. *The Cryosphere*, *6*(4), 821–839. https://doi.org/10.5194/tc-6-821-2012

Caesar, L., Rahmstorf, S., Robinson, A., Feulner, G., & Saba, V. (2018). Observed fingerprint of a weakening Atlantic Ocean overturning circulation. *Nature Climate Change*, *556*, 191–196. https://doi.org/10.1038/s41586-018-0006-5

Ciraci, E., Velicogna, I., & Swenson, S. (2020). Continuity of the mass loss of the World's glaciers and IceCaps from the GRACE and GRACE follow-on missions. *Geophysical Research Letters*, *47*(9), e2019GL086926. https://doi.org/10.1029/2019GL086926

Cogley, J., Hock, R., Rasmussen, L., Arendt, A., Bauder, A., Braithwaite, R., et al. (2011). Glossary of glacier mass balance and related terms. *IHP-VII Technical Documents in Hydrology No. 86, IACS Contribution No. 2*. Paris: UNESCO-IHP.

Dee, D. P., Uppala, S. M., Simmons, A. J., Berrisford, P., Poli, P., Kobayashi, S., et al. (2011). The ERA-Interim reanalysis: Configuration and performance of the data assimilation system. *Quarterly Journal of the Royal Meteorological Society*, *137*, 553–597. https://doi.org/10.1002/qj.828

ECMWF-IFS. (2008). *Part IV: PHYSICAL PROCESSES (CY33R1). Technical Report*.

Ettema, J., van den Broeke, M. R., van Meijgaard, E., van de Berg, W. J., Box, J. E., & Steffen, K. (2010). Climate of the Greenland ice sheet using a high-resolution climate model—Part 1: Evaluation. *The Cryosphere*, *4*, 511–527. https://doi.org/10.5194/tc-4-511-2010

Eyring, V., Bony, S., Meehl, G. A., Senior, C. A., Stevens, B., Stouffer, R. J., & Taylor, K. E. (2016). Overview of the Coupled Model Intercomparison Project Phase 6 (CMIP6) experimental design and organization. *Geoscientific Model Development*, *9*(5), 1937–1958. https://doi.org/10.5194/gmd-9-1937-2016

Farinotti, D., Huss, M., Fürst, J. J., Landmann, J., Machguth, H., Maussion, F., & Pandit, A. (2019). A consensus estimate for the ice thickness distribution of all glaciers on Earth. *Nature Geoscience*, *12*, 168–173. https://doi.org/10.1038/s41561-019-0300-3

Fausto, R. S., van As, D., Box, J. E., Colgan, W., Langen, P. L., & Mottram, R. H. (2016). The implication of nonradiative energy fluxes dominating Greenland ice sheet exceptional ablation area surface melt in 2012. *Geophysical Research Letters*, *43*(6), 2649–2658. https://doi.org/10.1002/2016GL067720

Foresta, L., Gourmelen, N., Pálsson, F., Nienow, P., Björnsson, H., & Shepherd, A. (2016). Surface elevation change and mass balance of Icelandic ice caps derived from swath mode CryoSat-2 altimetry. *Geophysical Research Letters*, *43*(23), 12138–12145. https://doi.org/10.1002/2016GL071485

Fox-Kemper, B., Hewitt, H. T., Xiao, C., Aðalgeirsdòttir, G., Drijfhout, S. S., Edwards, T. L., et al. (2021). Ocean, cryosphere and sea level change. In *Climate change 2021: The physical science basis. Contribution of working group I to the sixth assessment report of the intergovernmental panel on climate change*. IPCC.

Garcia-Mondéjar, A., Gourmelen, N., Escorihuela, M. J., Roca, M., Shepherd, A., & Plummer, S. (2019). Multisurface retracker for swath processing of interferometric radar altimetry. *IEEE Geoscience and Remote Sensing Letters*, *16*(12), 1839–1843. https://doi.org/10.1109/LGRS.2019.2913635

Gardner, A. S., Moholdt, G., Cogley, J. G., Wouters, B., Arendt, A. A., Wahr, J., et al. (2013). A reconciled estimate of glacier contributions to sea level rise: 2003 to 2009. *Science*, *340*(6134), 852–857. https://doi.org/10.1126/science.1234532

Gascoin, S., Guðmundsson, S., Aðalgeirsdóttir, G., Pálsson, F., Schmidt, L., Berthier, E., & Björnsson, H. (2017). Evaluation of MODIS albedo product over ice caps in Iceland and impact of volcanic eruptions on their albedo. *Remote Sensing*, *9*(399). https://doi.org/10.3390/rs9050399

Gervais, M., Shaman, J., & Kushnir, Y. (2018). Mechanisms governing the development of the north Atlantic warming hole in the CESM-LE future climate simulations. *American Meteorological Society*, *31*(15), 5927–5946. https://doi.org/10.1175/JCLI-D-17-0635.1

Gettelman, A., Truesdale, J. E., Bacmeister, J. T., Caldwell, P. M., Neale, R. B., Bogenschutz, P. A., & Simpson, I. R. (2019). The Single Column Atmosphere Model Version 6 (SCAM6): Not a scam but a tool for model evaluation and development. *Journal of Advances in Modeling Earth Systems*, *11*(5), 1381–1401. https://doi.org/10.1029/2018MS001578

Gudmundsson, M. T., Thordarson, T., Höskuldsson, Á., Larsen, G., Björnsson, H., Prata, F. J., et al. (2012). Ash generation and distribution from the April-May 2010 eruption of Eyjafjallajökull, Iceland. *Scientific Reports*, *2*(572), 12. https://doi.org/10.1038/srep00572

Gunnarsson, A., Gardarsson, S. M., Pálsson, F., Jóhannesson, T., & Sveinsson, Ó. G. B. (2021). Annual and inter-annual variability and trends of albedo of Icelandic glaciers. *The Cryosphere*, *15*(2), 547–570. https://doi.org/10.5194/tc-15-547-2021

Hersbach, H., Bell, B., Berrisford, P., Hirahara, S., Horànyi, A., Munoz-Sabater, J., et al. (2020). The ERA5 global reanalysis. *Quarterly Journal of the Royal Meteorological Society*, *146*(730), 1999–2049. https://doi.org/10.1002/qj.3803

Hock, R., Rasul, G., Adler, C., Cáceres, B., Gruber, S., Hirabayashi, Y., et al. (2019). High mountain areas. In *IPCC special report on the ocean and cryosphere in a changing climate*. IPCC SROCC.

Jacob, T., Wahr, J., Pfeffer, W. T., & Swenson, S. (2012). Recent contributions of glaciers and ice caps to sea level rise. *Nature*, *514*(482), 514–518. https://doi.org/10.1038/nature10847

Jóhannesson, T., Pálmason, B., Hjartarson, A., Jarosch, A. H., Magnússon, E., Belart, J. M. C., & Gudmundsson, M. T. (2020). Non-surface mass balance of glaciers in Iceland. *Journal of Glaciology*, *66*(258), 685–697. https://doi.org/10.1017/jog.2020.37

Josey, S. A., Hirschi, J. J.-M., Sinha, B., Duchez, A., Grist, J. P., & Marsh, R. (2017). The recent Atlantic cold anomaly: Causes, consequences, and related phenomena. *Annual Reviews of Marine Science*, *10*, 475–501. https://doi.org/10.1146/annurev-marine-121916-063102

Keil, P., Mauritsen, T., Jungclaus, J., Hedemann, C., Olonscheck, D., & Ghosh, R. (2020). Multiple drivers of the North Atlantic warming hole. *Nature Climate Change*, *10*, 667–671. https://doi.org/10.1038/s41558-020-0819-8

Lawrence, D. M., Fisher, R. A., Koven, C. D., Oleson, K. W., Swenson, S. C., Bonan, G., et al. (2019). The Community Land Model version 5: Description of new features, benchmarking, and impact of forcing uncertainty. *Journal of Advances in Modeling Earth Systems*, *11*(12), 4245–4287. https://doi.org/10.1029/2018MS001583

Lenaerts, J. T. M., van den Broeke, M. R., Angelen, J. H., van Meijgaard, E., & Déry, S. J. (2012). Drifting snow climate of the Greenland ice sheet: A study with a regional climate model. *The Cryosphere*, *6*, 891–899. https://doi.org/10.5194/tc-6-891-2012

Ligtenberg, S. R. M., Helsen, M. M., & van den Broeke, M. R. (2011). An improved semi-empirical model for the densification of Antarctic firn. *The Cryosphere*, *5*, 809–819. https://doi.org/10.5194/tc-5-809-2011

Ligtenberg, S. R. M., Munneke, P. K., Noël, B., & van den Broeke, M. R. (2018). Brief communication: Improved simulation of the present-day Greenland firn layer (1960-2016). *The Cryosphere*, *12*(5), 1643–1649. https://doi.org/10.5194/tc-12-1643-2018

Lipscomb, W. H., Price, S. F., Hoffman, M. J., Leguy, G. R., Bennett, A. R., Bradley, S. L., et al. (2019). Description and evaluation of the community ice sheet model (CISM) v2.1. *Geoscientific Model Development*, *12*(1), 387–424. https://doi.org/10.5194/gmd-12-387-2019

Meredith, M., Sommerkorn, M., Cassotta, S., Derksen, C., Ekaykin, A., Hollowed, A., et al. (2019). Polar regions. In *IPCC special report on the ocean and cryosphere in a changing climate*. IPCC SROCC.

Möller, R., Dagsson-Waldhauserova, P., Möller, M., Kukla, P. A., Schneider, C., & Gudmundsson, M. T. (2019). Persistent albedo reduction on southern Icelandic glaciers due to ashfall from the 2010 Eyjafjallajökull eruption. *Remote Sensing of Environment*, *23*, 111396. https://doi.org/10.1016/j.rse.2019.111396

Nilsson, J., Sørensen, L. S., Barletta, V. R., & Forsberg, R. (2015). Mass changes in Arctic ice caps and glaciers: Implications of regionalizing elevation changes. *The Cryosphere*, *9*(1), 139–150. https://doi.org/10.5194/tc-9-139-2015

Noël, B., van de Berg, W. J., Lhermitte, S., & van den Broeke, M. R. (2019). Rapid ablation zone expansion amplifies north Greenland mass loss. *Science Advances*, *5*(9), eaaw0123. https://doi.org/10.1126/sciadv.aaw0123

Noël, B., van de Berg, W. J., Machguth, H., Lhermitte, S., Howat, I., Fettweis, X., & van den Broeke, M. R. (2016). A daily, 1 km resolution data set of downscaled Greenland ice sheet surface mass balance (1958–2015). *The Cryosphere*, *10*(5), 2361–2377. https://doi.org/10.5194/tc-10-2361-2016

Noël, B., van de Berg, W. J., van Meijgaard, E., Munneke, P. K., van de Wal, R. S. W., & van den Broeke, M. (2015). Evaluation of the updated regional climate model RACMO2.3: Summer snowfall impact on the Greenland ice sheet. *The Cryosphere*, *9*, 1831–1844. https://doi.org/10.5194/tc-9-1831-2015

Noël, B., van Kampenhout, L., Lenaerts, J. T. M., van de Berg, W. J., & van den Broeke, M. R. (2021). A 21st century warming threshold for sustained Greenland ice sheet mass loss. *Geophysical Research Letters*, *48*(5), e2020GL090471. https://doi.org/10.1029/2020GL090471

Pálsson, F., Gunnarsson, A., Jónsson, G., Pálsson, H. S., & Steinpórsson, S. (2020). *Vatnajökull: Mass balance, meltwater drainage and surface velocity of the glacial year 2018–19*. Institute of Earth Sciences University of Iceland and National Power Company.

Porter, C., Morin, P., Howat, I., Noh, M.-J., Bates, B., Peterman, K., et al. (2018). *ArcticDEM. Harvard Dataverse*. https://doi.org/10.7910/DVN/OHHUKH

Rahmstorf, S., Box, J. E., Feulner, G., Mann, M. E., Robinson, A., Rutherford, S., & Schaffernicht, E. J. (2015). Exceptional twentieth-century slowdown in Atlantic Ocean overturning circulation. *Nature*, *5*, 475–480. https://doi.org/10.1038/nclimate2554

RGI Consortium. (2017). Randolph Glacier Inventory—A dataset of global glacier outlines: Version 6.0. Technical Report. *Global land ice measurements from space*. https://doi.org/10.7265/N5-RGI-60

Schmidt, L. S., Aðalgeirsdóttir, G., Guðmundsson, S., Langen, P. L., Pálsson, F., Mottram, R., et al. (2017). The importance of accurate glacier albedo for estimates of surface mass balance on Vatnajökull: Evaluating the surface energy budget in a regional climate model with automatic weather station observations. *The Cryosphere*, *11*(4), 1165–1184. https://doi.org/10.5194/tc-11-1665-2017

Schrama, E., Wouters, B., & Rietbroek, R. (2014). A mascon approach to assess ice sheet and glacier mass balances and their uncertainties from GRACE data. *Journal of Geophysical Research*, *119*(7), 6048–6066. https://doi.org/10.1002/2013JB010923

Siemes, C., Ditmar, P., Riva, R. E. M., Slobbe, D. C., Liu, X. L., & Farahani, H. H. (2013). Estimation of mass change trends in the Earth's system on the basis of GRACE satellite data, with application to Greenland. *Journal of Geodesy*, *87*, 69–87. https://doi.org/10.1007/s00190-012-0580-5

Smith, R., Jones, P., Briegleb, B., Bryan, F., Danabasoglu, G., Dennis, J., et al. (2010). The parallel ocean program (POP) reference manual ocean component of the community climate system model (CCSM) and community earth system model (CESM). *Report LAUR-01853*, *141*, 1–140.

Sørensen, L. S., Jarosch, A. H., Aðalgeirsdóttir, G., Barletta, V. R., Forsberg, R., Pálsson, F., et al. (2017). The effect of signal leakage and glacial isostatic rebound on GRACE-derived ice mass changes in Iceland. *Geophysical Journal International*, *209*(1), 226–233. https://doi.org/10.1093/gji/ggx008

Undèn, P., Rontu, L., Järvinen, H., Lynch, P., Calvo, J., Cats, G., et al. (2002). *HIRLAM-5. Scientific Documentation* (Technical Report).

Uppala, S. M., Kållberg, P. W., Simmons, A. J., Andrae, U., Bechtold, V. D. C., Fiorino, M., et al. (2005). The ERA-40 re-analysis. *Quarterly Journal of the Royal Meteorological Society*, *131*, 2961–3012.

Van Angelen, J. H., Lenaerts, J. T. M., Lhermitte, S., Fettweis, X., Munneke, P. K., van den Broeke, M. R., et al. (2012). Sensitivity of Greenland ice sheet surface mass balance to surface albedo parameterization: A study with a regional climate model. *The Cryosphere*, *6*, 1175–1186. https://doi.org/10.5194/tc-6-1175-2012

Van de Berg, W. J., & Medley, B. (2016). Brief Communication: Upper-air relaxation in RACMO2 significantly improves modelled interannual surface mass balance variability in Antarctica. *The Cryosphere*, *10*, 459–463. https://doi.org/10.5194/tc-10-459-2016

Von Hippel, M., & Harig, C. (2019). Long-term and inter-annual mass changes in the Iceland ice cap determined from GRACE gravity using Slepian functions. *Frontiers in Earth Science*, *7*(171), 1–10. https://doi.org/10.3389/feart.2019.00171

Wouters, B., Chambers, D., & Schrama, E. J. O. (2008). GRACE observes small-scale mass loss in Greenland. *Geophysical Research Letters*, *35*(20), L20501. https://doi.org/10.1029/2008GL034816

Wouters, B., Gardner, A., & Moholdt, G. (2019). Global glacier mass loss during the GRACE satellite mission (2002–2016). *Frontiers in Earth Sicence*, *7*(96), 11. https://doi.org/10.3389/feart.2019.00096

Zemp, M., Huss, M., Thibert, E., Eckert, N., McNabb, R., Huber, J., et al. (2019). Global glacier mass changes and their contributions to sea-level rise from 1961 to 2016. *Nature*, *568*, 382–386. https://doi.org/10.1038/s41586-019-1071-0

Zhu, C., & Liu, Z. (2020). Weakening Atlantic overturning circulation causes South Atlantic salinity pile-up. *Nature Climate Change*, *10*, 998–1003. https://doi.org/10.1038/s41558-020-0897-7